UNDERSTANDING AND MODELLING VARIABILITY IN MODULUS AND STRENGTH OF TOW-BASED DISCONTINUOUS COMPOSITES

Yizhuo Li[1], Soraia Pimenta[1], Jordan Singgih[1], Charlotte Ottenwelter[1], Stefan Nothdurfter[2], Karsten Schuffenhauer[2]

[1]meComposites, Department of Mechanical Engineering, Imperial College London, South Kensington Campus, London, SW7 2AZ, UK
[2]Automobili Lamborghini S.p.A. Advanced Composite Research Center, Via Modena 12, 40019 Sant'Agata Bolognese (BO), Italy
Email: yizhuo.li10@imperial.ac.uk

Keywords: Discontinuous composites, Equivalent laminate, Statistical variability, Mechanical properties, FE simulations

ABSTRACT

Tow-based discontinuous composites (TBDCs) are a growing class of high performance lightweight discontinuous composites, suitable for structural applications in the automotive industry. TBDCs consist of a network of randomly placed and oriented tows; this microstructure allows TBDCs to combine high specific modulus and toughness low manufacturing time and cost. However, this microstructure also leads to highly heterogeneous microstructures and properties in TBDCs, which makes it difficult to predict the mechanical response of these materials, especially in structural components with complex geometries. Therefore, this study aims to quantify the effect of the intrinsic variability of mechanical properties of TBDCs, and to develop a design framework that can be used for structural design with these materials. This study aims to understand the variability of the TBDCs, and to develop a design framework that can be used for structural design with these materials. This is achieved by (i) experimentally quantifying the effect of the intrinsic variability in microstructure on the mechanical properties of TBDCs; (ii) developing analytical models to predict the mechanical properties of TBDCs according to their local microstructure and their variability; and (iii) integrating the distribution of mechanical properties calculated from the analytical models into a finite element environment to simulate the mechanical response of a structure under load. It is found that the variability in TBDCs is so significant that the critical regions in a structure can be shifted to other locations, even with substantial stress concentrations. It is also shown that the analytical models and the FE design framework proposed in this study can be used to optimise the microstructure of TBDCs and to design structures using TBDCs, hence accelerating the design cycle and promoting the application of high-performance composites in high-volume applications.

1 INTRODUCTION

Light-weight carbon-fibre composites are now widely-used in the aircraft industry, and contribute to a reduction of fuel consumption and carbon-footprints in air transportation. A simlar penetration of carbon-fibre composites in the automotive industry could lead to a reduction of 60 Mton of CO_2 emissions per year [1]; however, the use of carbon-fibre composites has been limited to the high-end automotive sector due to their high manufacturing cost. Therefore, there is an urgent challenge to develop cheaper carbon-fibre composites and broaden their application to high-volume production industries.

This challenge can be addressed by promoting the use of carbon-fibre Tow-Based Discontinuous Composites (TBDCs), which consist of a network of randomly-located and randomly-oriented carbon-fibre tows embedded in a polymeric matrix. Due to the discontinuous nature of the tows, TBDCs can be compression-moulded, which significantly reduces their manufacturing time (down to 2 min using

fast-curing epoxies) and cost (down by 40%), compared to conventional continuous-fibre composites. Moreover, TBDCs can be moulded into complex shapes with built-in ribs and connectors, which can further reduce the weight of structures and assembly time.

The tow-based architecture of TBDCs allows for higher fibre-content (up tp 60%), leading to high modulus (20-60 GPa), moderate strength (150-500 MPa), and high toughness (65-100 kJ/m^2) [2–4]. These advantages have already been exploited in the window frames of the 787 Dreamliner, the inner monocoque and suspension control arm of the 'Sesto Elemento' concept car from Automobili Lamborghini, and the Diablo Octane drivers from Callaway Golf, but could be further extended to (for instance) the mainstream automotive industry.

A noticeable feature of TBDCs is that their microstructure is highly heterogeneous, due to the large tow dimensions (up to 50 mm long and 10 mm wide) and random tow orientations. This results in variability of local properties and in the presence of internal weak spots in TBDCs, which makes these materials notch insensitive [5]. Although notch insensitivity is advantageous for structural applications, it showcases that the heterogeneous microstructure and variability of properties in TBDCs have a significant impact on their mechanical performance, and must therefore be accounted for in structural design.

There are few models in the literature to predict modulus and strength of TBDCs while accounting for their heterogeneous microstructure. Feraboli *et al.* have developed an FE framework to predict the stress-strain response of TBDCs considering heterogeneous modulus fields, but this framework is not able to predict failure of a structure [6]. Harper *et al.* developed an FE model which represents the tows explicitly in a random microstructure, and considers a combination of maximum stress criterion for fibre failure and von Mises for matrix failure [7]; however, such model is computationally very expensive, and cannot therefore be used to model a full-sized structural component made with TBDCs. Selezneva *et al.* proposed a model which defines the position of each tow for a whole structure, and considers Hashin's criterion for the failure of the local laminates at each point [8]; however, this model is also computationally-heavy, and uses a failure criterion which is suitable for continuous composites but does not account for the interaction between longitudinal and transverse failure modes which may happen in discontinuous composites.

Therefore, this study aims to develop a modelling framework to accelerate the design cycle with TBDCs, considering their intrinsic variability. This is achieved through the following objectives: (i) experimentally quantifying the effect of variability of the microstructure of TBDCs on their mechanical properties (Section 2); (ii) developing computationally-efficient analytical models to predict stochastic modulus and strength distributions for TBDCs (Section 3); and (iii) integrating the predicted stochastic properties into a Finite Element (FE) design tool, to predict the structural response of complex components, considering the spatial variability in modulus and strength (Section 4). Results are discussed in Section 5, and the main conclusions are drawn in Section 6.

2 CHARACTERISING THE SPATIAL VARIABILITY OF PROPERTIES IN TBDCS

2.1 Manufacturing and testing equivalent laminates and random composites

To quantify the effect of the microstructural variability on the mechanical properties of TBDCs, two types of tow-based discontinuous composite plates were manufactured:

1. Random Composite (RC) plates, made of chopped prepreg *tows* randomly oriented and distributed in a plate (Figure 1a), mimicking the heterogeneous microstructure and variability of actual TBDCs;
2. Equivalent Laminate (EL) plates, with a Quasi-Isotropic (QI) lay-up of Uni-Directional (UD) prepreg plies, where each UD ply has cuts defining aligned tows (see Figure 1b); this removes the spatial variability found in RCs, while preserving the discontinuous and tow-based nature of the microstructure.

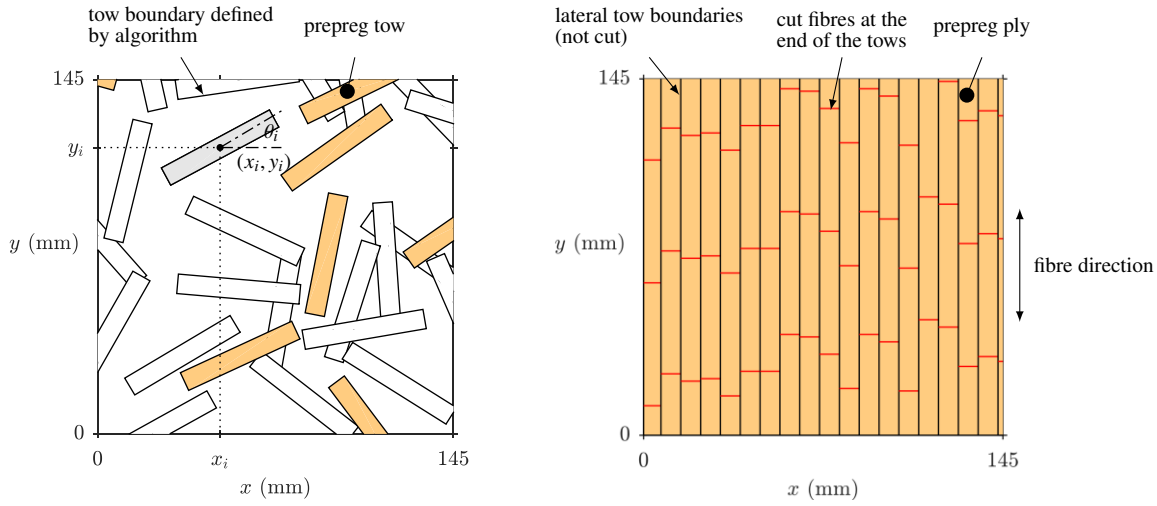

(a) Layer with randomly distributed tows in the RC. (b) UD ply with aligned discontinuous tows in the EL.

Figure 1: Examples of patterns of tow boundaries in RC and EL layers generated by the randomisation algorithms. Both figures represent a quarter of the full plates manufactured (290×290 mm^2).

The same tow dimensions and prepreg materials (defined in Table 1) were used in both the RC and EL plates; two RC plates and two EL plates were made, using prepregs of thickness $t_t = 0.164$ mm (later referred to as 'thin-prepreg') or $t_t = 0.285$ mm (later referred to as 'thick-prepreg'). The number of tows in the thin- and thick-prepreg RC plates were selected to be the same as in their corresponding EL plates.

To manufacture the RC plates, a randomisation algorithm was used to realise the position (x_i, y_i) and the orientation (θ_i) of each tow i as shown in Figure 1a. The tows were cut with an automated ply-cutter, and manually placed on the plate, one-by-one, according to the position (x_i, y_i) and orientation (θ_i) previously defined.

To manufacture the EL, a randomisation algorithm was used to realise the location of the tow boundaries in each uni-directional (UD) ply (see Figure 1b). An automated ply-cutter was used to generate the discontinuities perpendicular to the fibre direction. The UD plies were then laid-up into a quasi-isotropic laminate.

A hot press was used to cure the RC and EL plates, under a pressure of 5 bar and a temperature of 130 °C, for 20 min (as suggested by the manufacturer [9]). The modulus and strength of the RCs and ELs were characterised through standard uni-axial tensile tests, performed following the ASTM-D3039 [11] standard, but increasing the specimen width from the suggested 25 mm to the tow length of 50 mm.

Table 1: Tow dimension and properties of the UD composite (HexPly-M77 [9]) used to manufacture EL and RC plates.

Tow length l_t (mm)	Tow width w_t (mm)	Longitudinal modulus E_1 (GPa)	Transverse modulus E_2 (GPa)	Shear modulus G_{12} (GPa)
50.0	8	140 ⋆	9.0 †	5.6 †
Poisson's ratio ν_{12}	**Longitudinal strength X^T (MPa)**	**Transverse strength Y^T (MPa)**	**Shear strength S (MPa)**	**Fracture toughness $\mathcal{G}_{IIc}$ (kJ/m^2)**
0.34 †	2400 ⋆	73 †	78 ⋆	0.8 †

⋆ Values taken from material data-sheet [9]; † Typical properties of carbon/epoxy composites [10]

2.2 Results

Figure 2a shows that the moduli of the EL and RC specimens are similar, and that their moduli are not affected by the two prepreg thicknesses used. In Figure 2b, both the thin-prepreg RC and EL specimens show higher strengths than their thick-prepreg counterparts; there is a significant (20%-30%) strength reduction from the ELs to the corresponding RCs, which shows that the variability of the microstructure in the RCs has a major impact on the mechanical response of the material, and must therefore be accounted for.

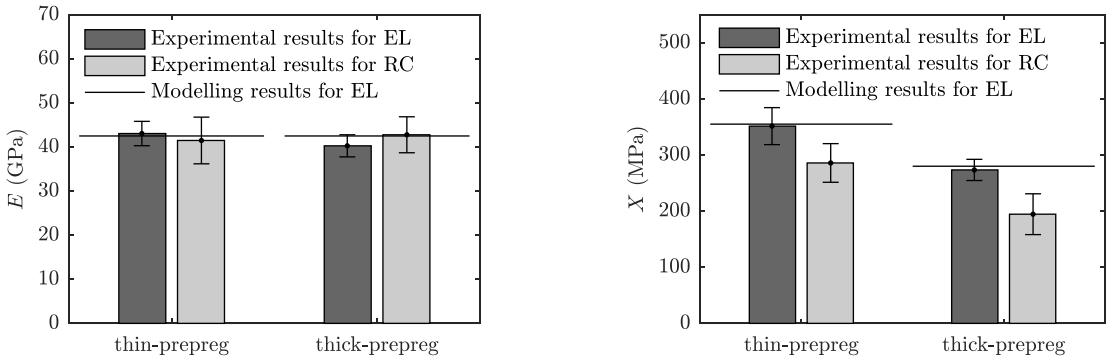

(a) Modulus of ELs and RCs.

(b) Tensile strength of ELs and RCs.

Figure 2: Experimentally measured modulus and strength of TBDCs, and modelling predictions.

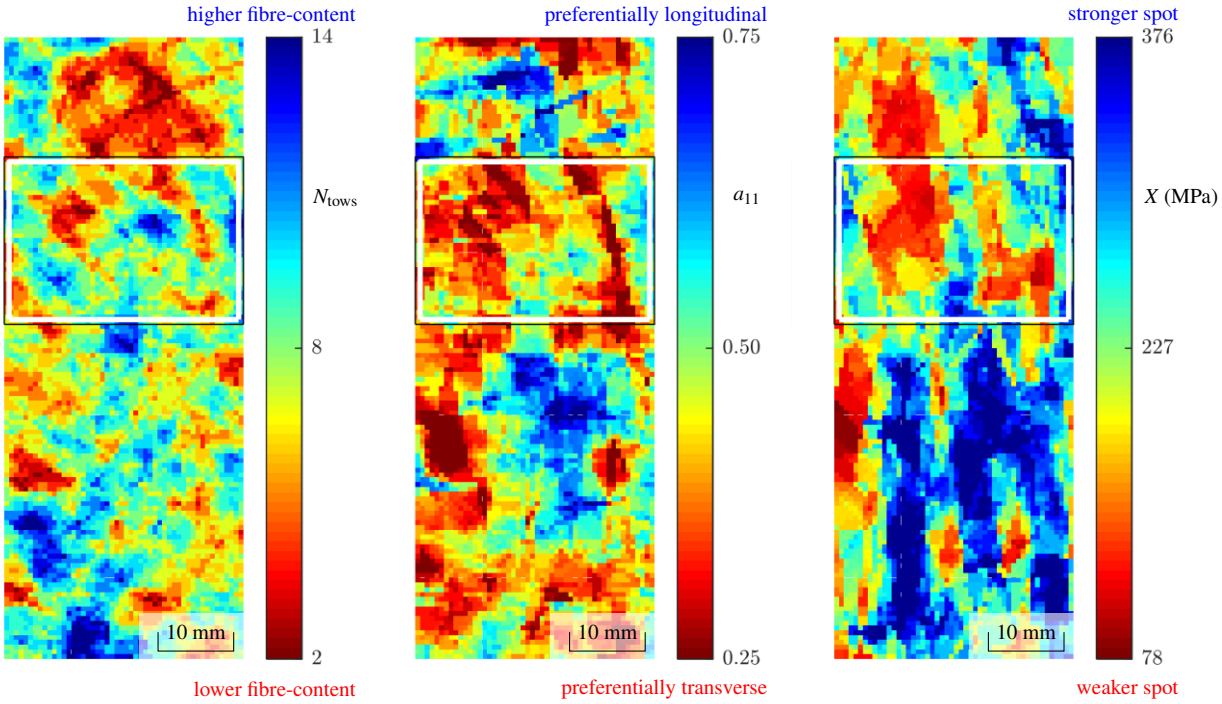

(a) Expected local number of tows.

(b) Expected local alignment parameter.

(c) Local strength predicted by the analytical model.

Figure 3: Expected characteristics of the local microstructure and predicted strength in the in-plane gauge section of one thick-prepreg specimen tested. The failure location is indicated by a black box.

Using the tow locations and orientations recorded by the randomisation algorithm used to make the RC plates (see Section 2.1), it was possible to calculate the expected map of the total number of tows (N_{tows}) present in the through-the-thickness direction of each RC plate; this map is shown for a specimen in Figure 3a. Similarly, it was possible to calculate the expected map of the local tow alignment parameter a_{11} at each point of the surface of a plate, defined as

$$a_{11} = \sum_{i=1}^{N_{\text{tows}}} \frac{\cos^2(\theta_i)}{N_{\text{tows}}}, \tag{1}$$

where θ_i is the orientation of tow i; this map is shown for the same specimen in Figure 3b. It has been experimentally verified that the expected microstructure was mostly preserved during the curing process [12], and therefore the maps shown in Figures 3a and 3b should be representative of the actual microstructure of the specimen tested experimentally. Failure of the specimen (identified in Figure 3a and Figure 3b) occurred in a region with low tow-count (small N_{tows}, corresponding to a low local fibre-content) and a preferential tow alignment transverse to the loading direction (low a_{11}), which correspond to a weak spot in the specimen. Similar trends were found in all 10 RC specimens tested, showing that the variability in the microstructure of RCs determines the failure location in the material.

3 ANALYTICAL MODULUS AND STRENGTH MODELS

3.1 Multi-scale framework based on the equivalent laminate assumption

Following from the experimental investigations in Section 2, this section proposes an analytical model to predict the modulus and strength of TBDCs based on the equivalent laminate analogy (see Figure 4), coupled with the stochastic variability of the microstructure of the material.

Considering that the TBDC is under plane-stress, the remote loading vector $\boldsymbol{\sigma}_{\text{g}}$ can be defined as:

$$\boldsymbol{\sigma}_{\text{g}} = [\sigma_x, \sigma_y, \tau_{xy}]^{\text{T}} = M \cdot \widehat{\boldsymbol{\sigma}}_{\text{g}}, \tag{2}$$

where $\widehat{\boldsymbol{\sigma}}_{\text{g}}$ defines a unit loading vector and M defines the magnitude of the applied load. The model then considers a multi-scale framework, as illustrated in Figure 4:

1. At the micro-scale (Figure 4a), the modulus (E_{D}) and strength (X_{D}^{T}) of a UD discontinuous ply with randomly-located tow-ends are calculated from a stochastic shear-lag model (Section 3.2);
2. At the meso-scale (Figure 4b), the model considers a ply with orientation θ; the unit loading vector of the ply ($\widehat{\boldsymbol{\sigma}}_{\theta}$) can be determined through classical laminate theory and assuming uniform local ($\boldsymbol{\varepsilon}_{\text{l}}$) and global ($\boldsymbol{\varepsilon}_{\text{g}}$) remote strain fields:
$$\widehat{\boldsymbol{\sigma}}_{\theta} = \boldsymbol{Q}_{\theta} \cdot \boldsymbol{\varepsilon}_{\text{l}} = \boldsymbol{Q}_{\theta} \cdot \boldsymbol{\varepsilon}_{\text{g}} = \boldsymbol{Q}_{\theta} \cdot (\boldsymbol{Q}_{\text{g}}^{-1} \widehat{\boldsymbol{\sigma}}_{\text{g}}), \tag{3}$$
where $\boldsymbol{Q}_{\text{g}}$ and $\boldsymbol{Q}_{\theta}$ are the global (laminate) and local (ply) modulus matrices respectively [13]. The key challenge of the meso-scale model is then to determine the failure envelope of the UD ply for a generic local unit loading vector $\widehat{\boldsymbol{\sigma}}_{\theta} = [\sigma_1, \sigma_2, \tau_{12}]^{\text{T}}$ (see Section 3.3);
3. At the macro-scale (Figure 4c), the model calculates the engineering constants, e.g. Young's modulus E_{g}, and the plane-stress failure envelopes (i.e. the critical magnitude M^* for any given unit loading vector $\hat{\boldsymbol{\sigma}}_{\boldsymbol{g}}$) of an equivalent laminate with a set of plies with different orientations.

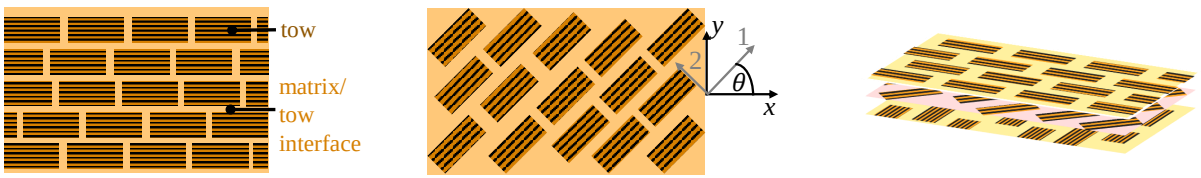

(a) UD ply

(b) UD discontinuous ply at θ orientation

(c) Equivalent laminate

Figure 4: Multi-scale architecture of TBDC used for modelling

3.2 Micro-scale

The micro-scale approach proposed here is based on the Stochastic extension of a non-linear Shear-Lag Model (SSLM) [14], assuming a bi-linear constitutive law at the interface between tows and a random placement of tow ends. Assuming a square arrangement of the tows in which each tow interacts with its 4 nearest neighbours, the model calculates the stress vs. strain curve of the UD ply as follows:

1. Calculating the stress-strain response $\sigma_o(\varepsilon_o; l_o; t_o)$ of each *overlap* defined between the ends of two neighbouring tows, which depends on the random tow overlap length $l_o \in [0, l_t]$ and random tow overlap thickness $t_o \in [0, t_t]$. This is calculated through a shear-lag model [14];
2. Calculating the stress-strain response of a single *tow*, considering that its stresses are built from the shear-lag overlaps with its four neighbours, and that the tow will break once its stresses reach the tow strength X^T;
3. Calculating the stress-strain curve of a *representative volume element (RVE)* containing a sufficiently large array of parallel tows.

The longitudinal tensile modulus (E_D) and longitudinal tensile strength (X_D^T) of the UD discontinuous ply are calculated from this stress-strain curve. The transverse and shear elastic properties are calculated from Halpin-Tsai's equations [15].

3.3 Meso-scale

The failure surface σ_1 vs. σ_2 vs. τ_{12} of a UD discontinuous ply is here calculated with a new Interactive Tension-Shear (ITS) criterion, which accounts for the interaction between longitudinal and shear loading observed in discontinuous composites. Consider a ply under an applied shear stress $|\tau_{12}| \leq S$ (where S is the shear strength); if this is superposed with a longitudinal tensile stress σ_1, the ability of the matrix to transfer stresses through shear-lag is now reduced to $S_{SL} = S - |\tau_{12}|$, and thus the maximum σ_1 allowed is lower than the value of X_D^T calculated in Section 3.2. By varying S_{SL} from 0 to S, a new σ_1 vs. τ_{12} failure envelope considering the interaction between longitudinal tensile failure and transverse shear failure is generated.

The matrix dominated (σ_2 vs. τ_{12}) failure envelope used at the meso-scale is based on LaRC05 [16]. Therefore, the interaction between σ_1 and τ_{12} described above is naturally extended to any combination of in-plane stresses, hence defining a longitudinal-transverse-shear failure surface as shown in Figure 5.

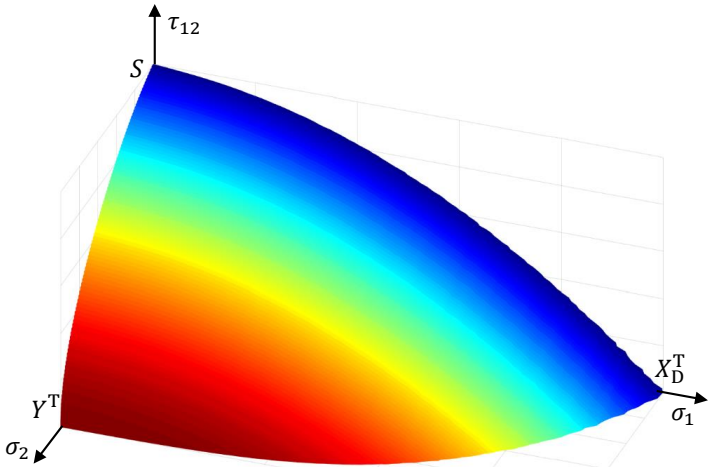

Figure 5: Longitudinal-transverse-shear failure surface determined from ITS criterion, for any UD discontinuous ply at orientation θ.

3.4 Macro-scale

Classical laminate theory is used to obtain the modulus matrix $\boldsymbol{Q}_{\mathrm{g}}$ of an equivalent laminate with N plies, with which the elastic properties of TBDCs can be extracted [13], as:

$$\boldsymbol{Q}_{\mathrm{g}} = \frac{\sum_{i=1}^{N} \boldsymbol{Q}_{\theta}}{N}. \tag{4}$$

A first ply failure criterion is used to calculate the strength of the equivalent laminate.

To predict the mean value of the modulus and strength of TBDCs, the equivalent laminate is assumed to have a quasi-isotropic lay-up with N plies, with an orientation off-set of $\theta_i = i \cdot \pi / N$ between each ply.

To account for the variability in the microstructure of TBDCs, a stochastic model considers a distribution of the number of plies N, and assigns a random orientation θ to each ply in the equivalent laminate is implemented.

3.5 Results

Figure 2 compares the modulus and strength predicted by the deterministic model (considering a quasi-isotropic equivalent laminate) against experimental results. Figure 2a shows good agreement between the modelling and experimental values of modulus, for both ELs and RCs. Figure 2b shows a very good agreement between the strength predicted for an equivalent laminate and the experimental data for EL; the model is also capable of capturing the effect of prepreg-thickness on the strength of TBDCs. However, as variability has not been accounted for in the deterministic model, there is a discrepancy of 20% - 30% between the modelling values and the experimental strengths of the RC specimens.

By plugging the local heterogeneous microstructure – i.e. the local number of N_{tows} and the tow orientations θ_i (Figure 3a and 3b) of the specimens tested in Section 2 – into the stochastic strength model, local strength maps of the same specimens can be generated, as shown in Figure 3c. It is shown that, at the failure region of the specimen, a lower-than-average strength is expected, and therefore the model could be used to predict the failure location of TBDCs according to their microstructure.

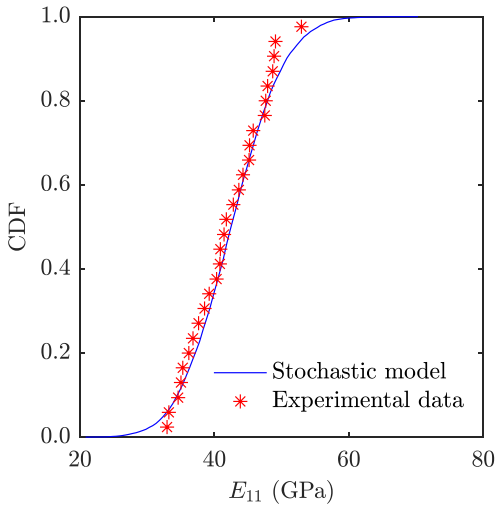

(a) CDF of modulus, experimental data and inputs for the model were taken from [17].

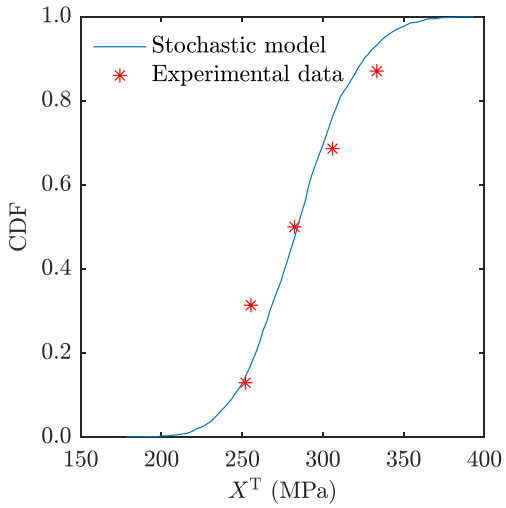

(b) CDF of strength.

Figure 6: The experimentally-measured and model-predicted cumulative density function (CDF) for the modulus and strength of TBDCs.

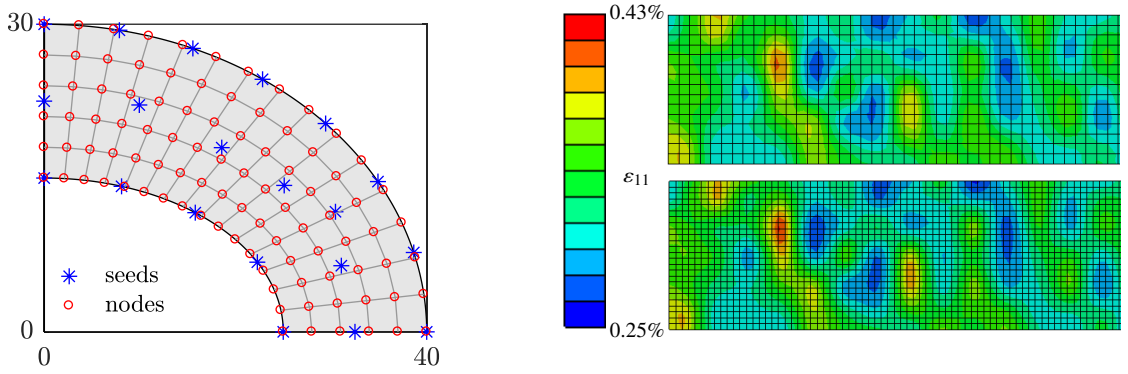

(a) Representation of seeds and nodes on a FE model (dimensions in mm).

(b) Mesh independence of the strain field on a plate under uniaxial tension (for the same realisation of seed properties).

Figure 7: Method to achieve mesh-independent property fields in the FE framework.

Another interesting prediction from the model is that, by increasing the thickness of the tows in a TBDC specimen, not only the average strength of the material decreases, but also the variability of the modulus and strength at each point of the microstructure increases. This also agrees with the experimental findings from Section 2, and further explains the more significant strength drop from EL to RC for the thick-prepreg than for the thin-prepreg.

Figure 6 shows the cumulative density function of the modulus and strength of TBDCs (considering the tow/prepreg thickness t_t = 0.164 mm), obtained by running the stochastic model for 10,000 realisations. The mean value and variability predicted by the model for both modulus and strength show good agreement with the experimental data.

4 FE IMPLEMENTATION TO ACCOUNT FOR VARIABLE MECHANICAL PROPERTIES

4.1 Mesh-independent stochastic property fields

The heterogeneous mechanical properties (modulus and strength) of TBDCs are mapped onto structural components at characteristic points referred to as *property seeds*. The spacing between these property seeds is defined as the tow width w_t [17]. The properties at the seeds are later interpolated to the *nodes* of the actual FE analysis mesh (see Figure 7a). This implementation ensures that the property fields assigned, and hence the stress/strain response calculated in FE, are mesh independent (see Figure 7b) [18].

4.2 Application to an automotive component

Variable modulus and strength fields (calculated based on the inputs in Table 1 and the model described in Section 3) are assigned to an automotive monocoque (approximately 2.07 m long and 1.73 m wide). The boundary conditions applied to the FE model are illustrated in Figure 8a).

Figure 8 shows the failure index distribution on the monocoque; the failure index was defined as the ratio between the local applied stress magnitude (M, see Equation 2) and the corresponding critical stress magnitude (M^*, see point 3 of Section 3.1).; the failure index was defined as the ratio between the local applied stress magnitude (M, see Equation 2) and the corresponding critical stress magnitude (M^*, see point 3 of Section 3.1). Figure 8a considers homogeneous properties of a QI equivalent laminate over the monocoque, and Figures 8b and 8c account for heterogeneous properties. In Figure 8b, the maximum failure index FI_{max} is found at the same location as in the homogeneous case, although with a magnitude 17% higher, implying that the actual monocoque with variable microstructure and properties

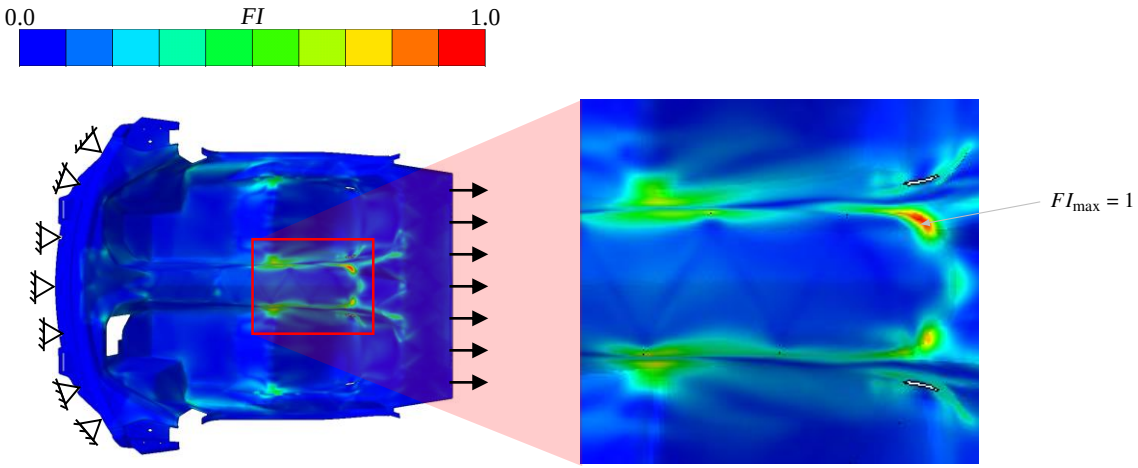

(a) BCs and FI field in a monocoque with homogeneous properties.

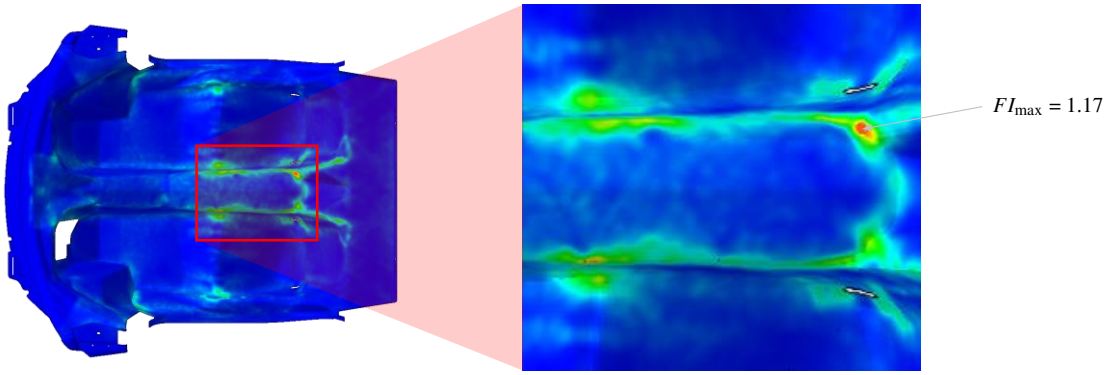

(b) Monocoque with heterogeneous property fields, showing a FI_{max} considerably higher than the homogeneous case.

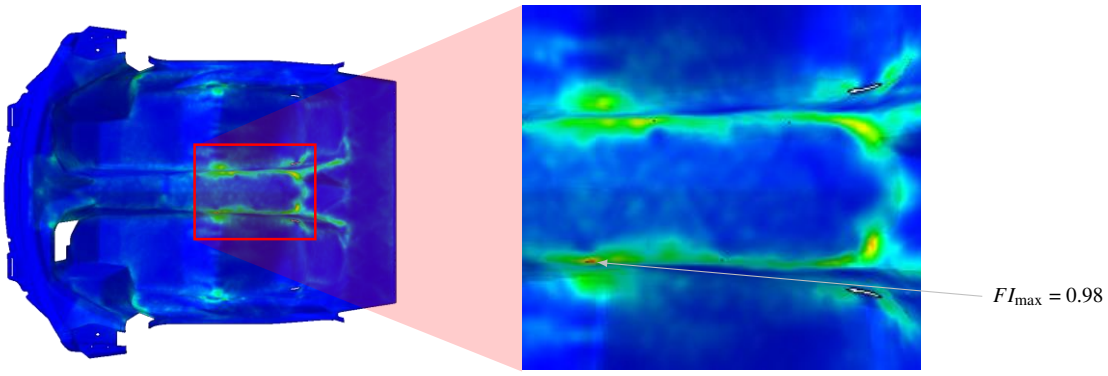

(c) Monocoque with heterogeneous property fields, showing a FI_{max} lower than the homogeneous case, and with the critical point shifted compared to the homogeneous case.

Figure 8: The failure index map of a monocoque predicted by FE, considering variability in modulus and strength fields.

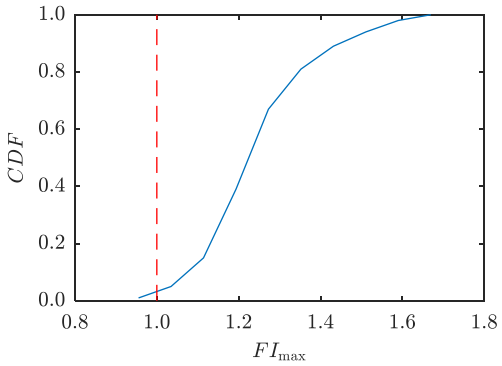

(a) Maximum failure index under the external load required to initiate failure in a monocoque with homogeneous properties corresponding to a QI equivalent laminate.

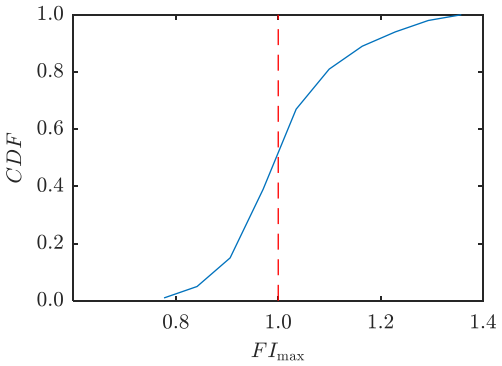

(b) Maximum failure index under the external load required to initiate failure in a monocoque with homogeneous properties corresponding to the average of random TBDC specimens.

Figure 9: Cumulative density function of maximum failure index in a monocoque with heterogeneous properties loaded in tension.

is likely to fail at a substantially lower applied external load. Figure 8c shows a different realisation where the location of the critical point has shifted, and the magnitude of $FI_{\max}$ is also smaller than that in the homogeneous case; this suggests that a different weak spot in the monocoque is more likely to fail prematurely.

Figure 9 shows the CDF for the maximum failure index in the monocoque, for a Monte-Carlo analysis with 100 runs; the Coefficient of Variation (CoV) is 31%. The external load applied to these runs corresponded to the load required to promote failure initiation (i.e. $FI_{\max} = 1$) in a baseline monocoque with homogeneous properties. In Figure 9a, these baseline homogeneous properties corresponded to those of a QI equivalent laminate; consequently, Figure 9a shows that a real monocoque is very likely to fail prematurely due to heterogeneities in its microstructure. In Figure 9b these baseline homogeneous properties correspond to the averages measured in random TBDC specimens; this shows that, for a real-life application, it would be necessary to apply a significant knock-down to the experimental averages when defining design allowables, in order to reduce the probability of reaching $FI_{\max} > 1$ in structures with heterogeneous properties.

5 DISCUSSION

5.1 Variability of TBDCs

The experimental investigation on randomly-oriented tow-based discontinuous composites and their equivalent ply-by-ply laminates shows that the variability when local fibre-content and local tow alignment in random TBDCs leads to a 20-30% reduction in the strength, when compared to their equivalent laminate counterparts (which shares the discontinuous architecture but have no variability in the microstructure). Moreover, a correlation between weak regions in the microstructure of the TBDCs (i.e. regions with lower fibre-content and preferential transverse tow alignment) and the location of failure has been observed (Figure 3), implying that the heterogeneity of TBDCs can change the location of critical points in a structure. Therefore, the localised variability of modulus and strength need to be accounted for when predicting the mechanical performance of TBDCs, specially when considered for structural applications.

When considering the variability of material properties in FE simulations of a monocoque, it is found that the critical failure index for a given applied load has a CoV of 12%. This suggests that a safety factor needs to be introduced when designing with TBDCs, to account for the potential local weakening due to the variability in the microstructure.

5.2 Material design

The analytical model proposed in this study indicates that, as the prepreg thickness of TBDCs increases, the dominating failure mechanism shifts from tow fracture to tow delamination; therefore, the model predicts a decrease in the average strength of TBDCs with increasing prepreg thickness.

Moreover, with a thicker tow/prepreg, the number of tows in the through-the-thickness direction in a plate decreases, and therefore the plate has a larger variability in the local fibre-content and local tow alignment parameter; consequently, the stochastic models predict that using thicker prepregs/tows leads to a larger variability in local modulus and strength, leading to an even lower failure strength of a specimen or a structure.

The model's capability to predict the effect of different microstructure on the mechanical performance of TBDCs hints for the potential to optimise the material by using thinner prepregs. The model can be further extended to optimise, for example, the tow length or the tow length-to-thickness aspect ratio for a better mechanical response, according the specifications of a given application.

5.3 Structural design

The Finite Element design tool proposed in this study is capable of simulating the response of a TBDC structure with a complex geometry, by generating mesh-independent modulus and strength field on the structure (considering the variability in the local fibre-content and tow orientation of TBDCs) and using failure criteria developed specifically for TBDCs.

It is shown that it is vital to consider this heterogeneity of TBDCs in structural design, not only because it has a significant effect on the allowable load (up to 11%) , but also because it is likely that the critical points of a structure can be shifted due to the local weakening created by the heterogeneous microstructure.

6 CONCLUSIONS

This work investigated the mechanical response of randomly-oriented tow-based discontinuous composites (TBDCs) and their equivalent laminates, and proposed analytical and FE models to predict the performance of TBDCs. The following conclusions can be drawn:

- This study shows that the variability of the microstructure in TBDCs is significant, leading up to 30% reduction in the strength, and potentially changing the location of the critical point in a structure;
- The analytical models developed to predict the modulus and strength of TBDCs, considering the intrinsic variability in the microstructure of these materials, provides accurate predictions for both the mean values and the variability of the modulus and the strength of TBDCs. It also provides guidance for designing the microstructure of TBDCs;
- The FE design tool developed to predict failure initiation in TBDC structures shows that, even in complex geometries with substantial geometric stress concentrations, the spatial variability of modulus and strength in TBDCs is likely to affect the maximum allowable load and the location of the critical point in the structure.

The design framework proposed in this study is helpful for broadening the application of TBDCs and accelerating their design cycle, hence promoting the use of these affordable composites in automotive and sporting industries.

ACKNOWLEDGEMENTS

S. Pimenta acknowledges the support from the Royal Academy of Engineering in the scope of her Research Fellowship on *Multiscale discontinuous composites for large scale and sustainable structural applications* (2015-2019).

REFERENCES

[1] SMMT motor industry facts 2016. Technical report, The society of motor manufacturers and traders, 2016.

[2] L. T. Harper et al. Characterisation of random carbon fibre composites from a directed fibre preforming process: Analysis of microstructural parameters. *Composites Part A*, 37(3):2136–2147, 2006.

[3] P. Feraboli et al. Characterization of prepreg-based discontinuous carbon fiber/epoxy systems. *J. Reinf. Plast. Compos.*, 28(10):1191–1214, 2009.

[4] S. Pimenta et al. Damage tolerant tow-based discontious composites. In *Proc. ICCM20*, 19-24 Jul 2015.

[5] C. Qian et al. Notched behaviour of discontinuous carbon fibre composites: Comparison with quasi-isotropic non-crimp fabric. *Composites Part A*, 42(3):293–302, 2011.

[6] P. Feraboli et al. Stochastic laminate analogy for simulating the variability in modulus of discontinuous composite materials. *Composites Part A*, 41:557–570, 2010.

[7] L. T. Harper et al. 3D geometric modelling of discontinuous fibre composites using a force-directed algorithm. *J. Compos. Mater.*, 0(0):1–18, 2016.

[8] M. Selezneva et al. Modelling of mechanical properties of randomly oriented strand thermoplastic composites. *J. Compos. Mater.*, 2017.

[9] Hexcel corporation. *HexPly–M77 Product Data*, Mar 2014. Accessed: 2017-01-30.

[10] S. S. Kaddour and M. J. Hinton. Maturity of 3D failure criteria for fibre-reinforced composites: Comparison between theories and experiments: Part B of WWFE-II. *J. Compos. Mater.*, 47:925–966, 2013.

[11] ASTM International. Standard test method for tensile properties of polymer matrix composite materials, ASTM D 3039/D 3039M – 07. In *Anual Book of ASTM Standards*, volume 08. 2008.

[12] Y. Li et al. Experimental investigation of randomly-oriented tow-based discontinuous composites and their equivalent laminates. *Composites Part A*, submitted (March 2017).

[13] S. W. Tsai and E. M. Wu. A general theory of strength for anisotropic materials. *J. Compos. Mater.*, 5:58–80, 1971.

[14] J Henry and S Pimenta. Semi-analytical simulation of aligned discontinuous composites. *Compos. Sci. Technol.*, 144:230–244, 2017.

[15] J. C. Halpin and J. L. Kardos. The Halpin-Tsai equations: a review. *Polym. Eng. Sci.*, 16(5):344–352, 1976.

[16] S. Pinho et al. Material and structural response of polymer-matrix fibre-reinforced composites. *J. Compos. Mater.*, 46:2313–2341, 2012.

[17] Feraboli et al. Modulus measurement for prepreg-based discontinuous carbon fiber/epoxy systems. *J. Compos. Mater.*, 43(19):1947–1965, 2009.

[18] Y. Li et al. Prediction of stiffness for tow-based discontinuous composites. In *Proc. ECCM17*, Munich, Germany, June 2016.